# THz Spectroscopy of Emerging Materials for Light Driven Processes and Energy Harvesting

Jens Neu<sup>a,b</sup>, Brian Pattengale<sup>a</sup>, Sarah Ostresh<sup>a</sup>, Matt D. Capobianco<sup>a</sup>, and Gary W. Brudvig<sup>a</sup>

<sup>a</sup>Yale University, Department of Chemistry, 225 Prospect Street, New Haven CT 06520 8107, USA

<sup>b</sup>Yale University, Department of Molecular Biophysics & Biochemistry, 266 Whitney Avenue, New Haven CT 06520 8114, USA

### **ABSTRACT**

Terahertz (THz) spectroscopy provides a crucial view on the electrical properties of emerging materials complementary to that which can be provided by more standard conductivity methods. The high frequency properties acquired in the THz range can be used to predict low frequency and DC behavior. THz spectroscopy provides insight into grain boundaries, phonon modes, and the underlying mechanism of charge transfer in general, paving the way towards superior design of novel materials. In this paper, we present pump-probe and time-domain THz spectroscopy on metal organic frameworks (MOFs) providing a detailed insight into carrier lifetime and charge scattering in MOFs.

Keywords: Terahertz (THz), Metal Organic Frameworks, Solar Energy Materials

#### 1. INTRODUCTION

Among the myriad challenges humanity is currently facing, the main challenge remains sustainability. Humans' insatiable hunger for energy depletes finite natural resources, creating a demand for novel materials which can be utilized to produce energy without exploiting scarce resources. Some of these scarce resources include rare metals, and thus a focus is placed on novel materials based on earth-abundant elements. While the reserves of coal and oil are getting smaller by the hour, the sunlight hitting our planet each hour would be sufficient to power humanity for more than one year. Tapping into this abundant resource is an ongoing endeavor. With efficiencies of silicon and other "simple" semiconductors pushed to its physical limit, higher efficiency demands novel materials.

The core challenge of solar energy is that it is intermittent. So apart from generating the energy, storing it efficiently is crucial to move towards full sustainability. One way is to use batteries to directly store electrical energy. These techniques usually exhibit moderate efficiency and demand large storage volume. Overcoming the volume issue can be achieved by storing solar energy chemically in stable molecules via catalysis. In such a scheme, the solar energy is used to create products, such as hydrogen, that can easily be converted into energy by electrochemical or combustion means.

There are two general strategies to harness solar energy for such catalytic energy storage schemes. One strategy is to use a solar cell to produce a voltage that can drive electrocatalysis at an appropriate electrode. While such a scheme has great potential, another strategy is to mimic natural photosynthesis by designing photocatalytic systems that directly uses light energy to drive photocatalysis. Such schemes have been termed "artificial photosynthesis", such as those aiming to split water into hydrogen and oxygen. In photocatalytic and electrocatalytic systems, increasing the amount of product produced is important to improve the overall solar fuel production. This led to interest in nanoparticles which have a large surface area that can be utilized for water splitting.<sup>1,2</sup> These nanoparticles can be decorated with catalytic and photo-harvesting materials (dyes).<sup>3</sup>

A promising improvement over nanoparticles are metal organic frameworks (MOFs). MOFs are microporous resulting in an even larger surface area than metal oxide nanoparticles. Furthermore, MOFs can be designed from

Send correspondence to

J.N.: E-mail: jens.neu@yale.edu, Telephone: +1 203-432-5045

a large set of different chemical compounds (pre-cursor) resulting in 75,600 MOFs in the last decades, representing 9~% of the largest crystallographic database (CCDC<sup>4</sup>). MOFs can be modified to incorporate photoactive and/or catalytic molecular species, and even more crucial some MOFs are conductive. Therefore, MOFs can harvest photoenergy, transfer photogenerated charges, and host catalytic centers in a highly porous framework. MOFs therefore provide an outstanding tool-kit to design novel photo-catalytical materials, combing flexibility in design with huge effective surface areas.

In this manuscript, we first discuss metal organic frameworks (MOFs). We then discuss how terahertz (THz) spectroscopy can be used to understand conductivity and photoconductivity in MOFs. We conclude by highlighting our recent work on MOFs.

# 2. METAL ORGANIC FRAMEWORK (MOF)

Metal organic frameworks (MOFs) are composed of metallic nodes that are connected with each other by organic linkers.<sup>5,6</sup> One of the MOFs studied is shown in Figure 1. The large free space (voids) in the structure are typical for MOFs and result in the huge active surface area.

The synthetic flexibility of MOFs inspired chemists to develop novel MOFs literally every day. For a MOF-based water-splitting solar cell, the MOF needs to be stable, porous, and incorporate catalytical centers and photo-absorbers. Ideally, the MOF would also have favorable charge-transport pathways (i.e. conductivity). In particular, conductivity is counterintuitive to porosity of the MOF. In general, electron transport in materials is governed by continuous energetically-degenerate states or bands. In MOFs, the organic ligands and nodes are spatially separated by the repeating structure such that an electron would need to overcome an energetic barrier in order for long-range transport to occur.

Recently several groups succeeded in fabrication of conductive MOFs.<sup>6</sup> Inspired by their promising results, we made a reported MOF derived from Mn<sub>2</sub>DSBDC.<sup>7</sup> The original MOF was found to be conductive previously, which was confirmed using THz spectroscopy for the first time for 3D MOF structures.<sup>5</sup> The same spectroscopic technique also confirmed the conductivity of cation-exchanged analogues that we have prepared and investigated in this work.

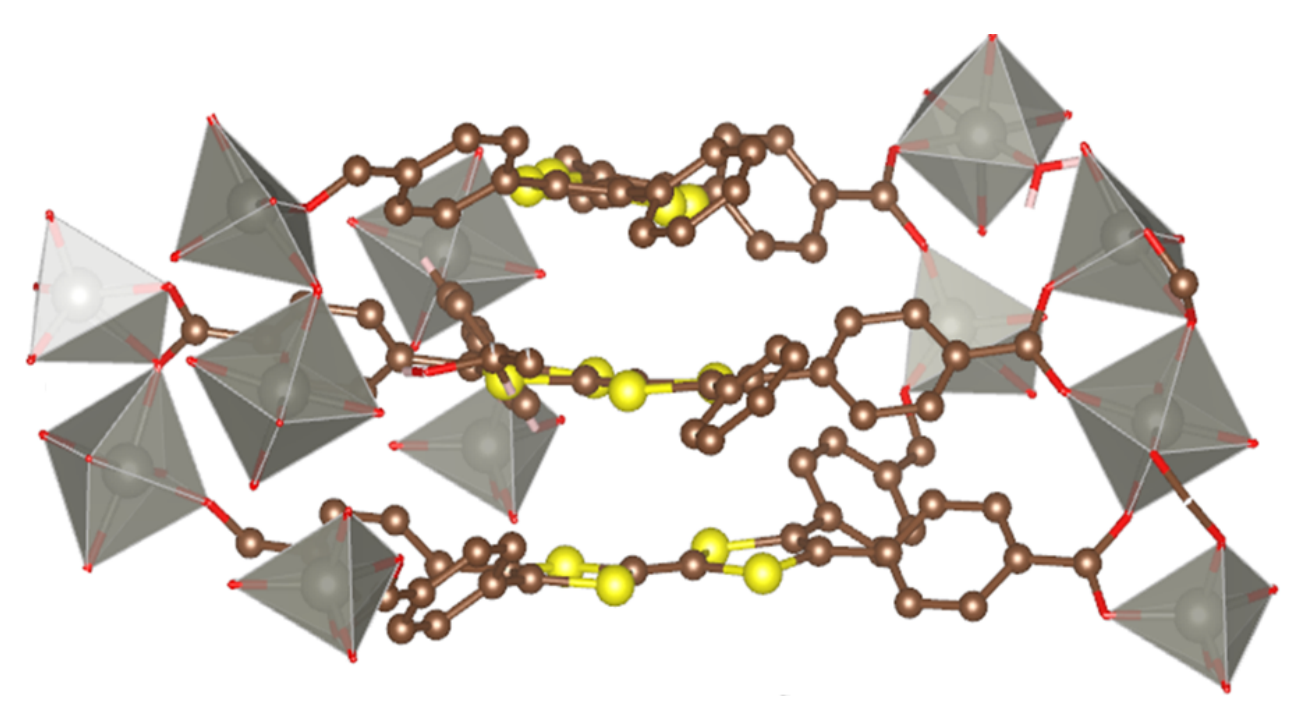


Figure 1. Structure of Zn<sub>2</sub>TTFTB. The yellow spheres depict sulfur linkages; the polyhedrons are caging the metal nodes.

# 2.1 Synthesis and Material Characterization of $Mn_2DSBDC$ and Cu-, Co- and Ni-Doped $Mn_2DSBDC$

Mn<sub>2</sub>DSBDC was synthesized as described in previous publication.<sup>8</sup> After synthesis about 10 % of the manganese in the MOF was replaced with Cu, Co, or Ni, respectively. For this process Mn<sub>2</sub>DSBDC was mixed with cobalt, copper, or nickel acetylacetonate, respectively. The mixture was heated to 100 °C under nitrogen atmosphere for 21 hours. The exchange or "dopant" metal diffused into the MOF replacing approximately 10 wt% of Mn from the original structure. X-ray diffraction (XRD) verified that the space group remained identical (Figure 2). The guest metal slightly shrunk the unit cell, compared to pristine Mn<sub>2</sub>DSBDC.

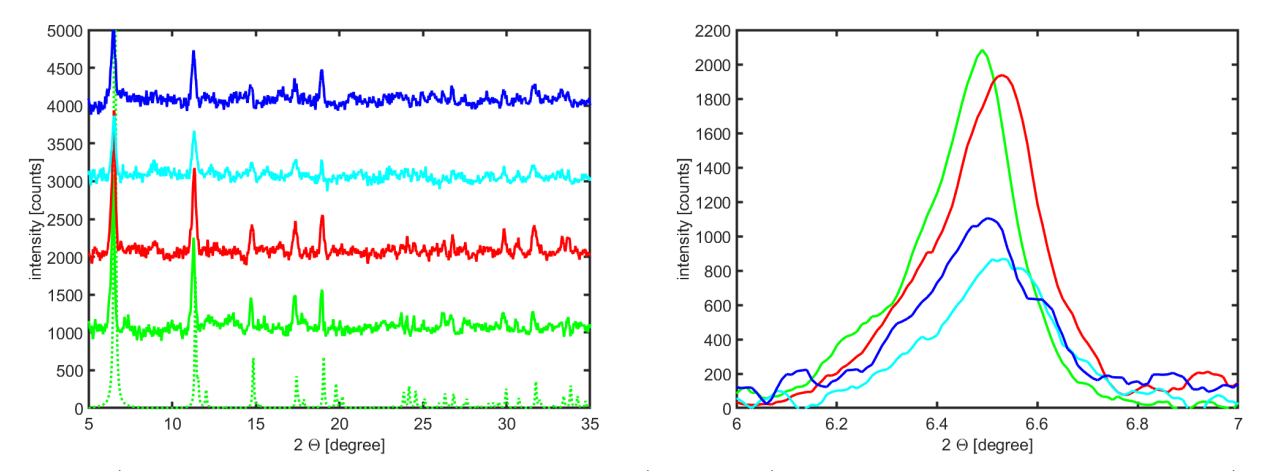


Figure 2. a) X-ray diffraction for the undoped  $Mn_2DSBDC$  (green, solid), computed for the  $Mn_2DSBDC$  structure (green, dashed), and for  $Mn_2DSBDC$  doped with the guest atoms Cu (red), Co (cyan), and Ni (blue). b) zoom at one peak illustrating the slight shrinkage induced by substitution of Mn by the guest atoms.

#### 3. THZ SPECTROSCOPY

The most crucial experiment related to conductive MOFs is measuring the conductivity of the synthesized material. This could be done via DC measurements.<sup>7</sup> However, these measurements present a crucial short coming; they need electrodes fabricated on the sample material. These contacts will introduce local contact effects and contact resistance complicating the interpretation of the measured DC-conductance. Furthermore, DC measurements are "long range", meaning the measured resistance is a combination of intra-grain and intergrain conductance. For a catalytical material, the inter-grain conductivity is rather unimportant, as dye and catalytical centers are both in the same grain. Even further complicating the issue, many MOFs have anisotropic charge transport throughout a given crystallographic grain in the form of one-dimensional or two-dimensional transport. Therefore, even if probes can be located on a single grain and the contact resistance can be accounted for, the measurement inherently cannot take into account this dimensionality in most cases because the probes can only measure the bulk property of the grain. As a result, DC measurements potentially underestimate the relevant conductivity in MOFs.

The best suited technique to measure intra-grain conductivity is Terahertz (THz) spectroscopy; in particular, THz-Time Domain Spectroscopy (THz-TDS). THz-TDS is a free-beam technique, so no contacts are needed. The material can be measured "as-is", in its powder form.

THz-TDS is based on measuring the THz electromagnetic field transmitted through the sample, referenced on a second measurement without the sample material. The big advantage of THz-TDS compared to most visible techniques is that THz-TDS detects the electrical component of the EM-field that is sign resolved with femtosecond resolution. The time traces carry all information of the EM-field, including amplitude and phase. In contrast to optical techniques which usually yield spectral intensity, THz-TDS provides amplitude and phase information. This information can be used to determine complex refractive indices of the sample material, without invoking the Kramers-Kronig relation or other concepts and approximations.

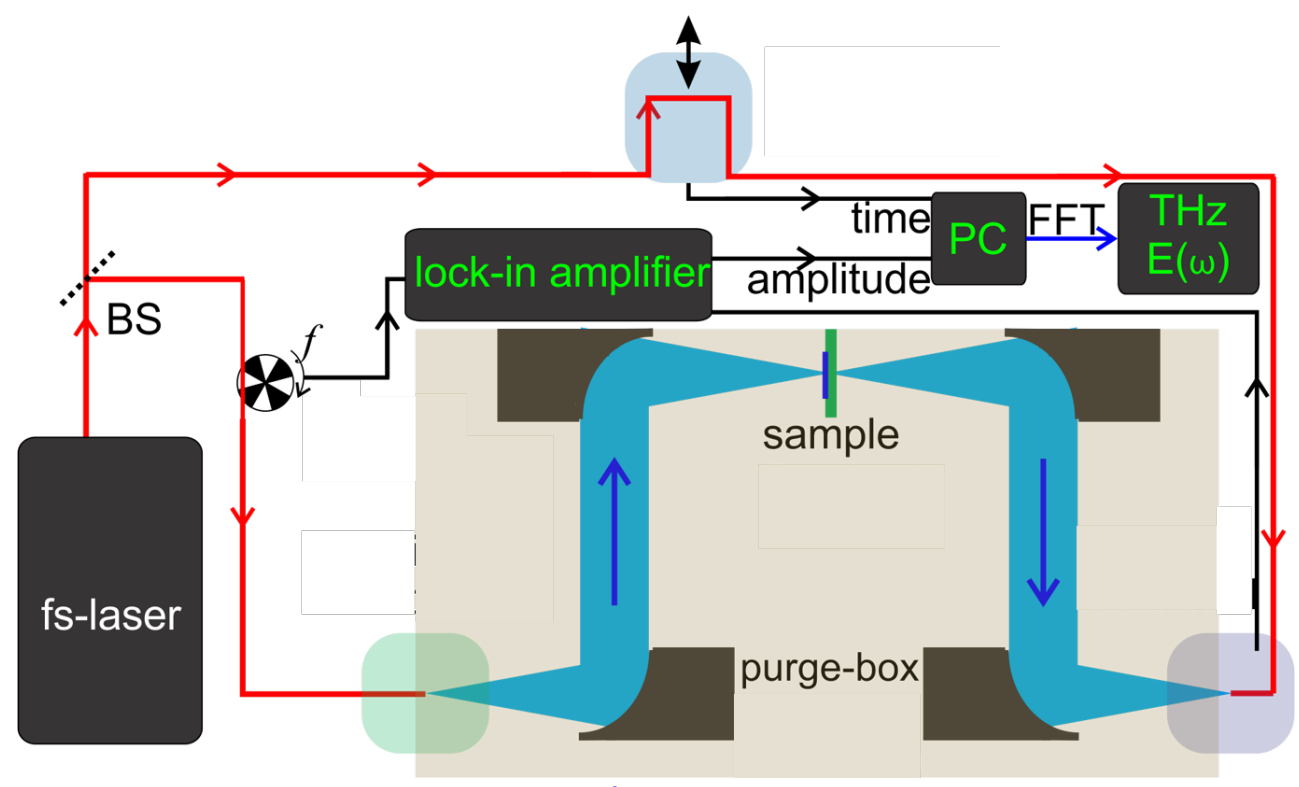


Figure 3. THz time domain spectrometers (adapted from<sup>9</sup>). The output of a femtosecond laser is split into THz generation and gate pulse (BS). The emission pulse is routed on a photoconductive switch to generate THz radiation. This radiation is guided using four off axis parabolic mirrors. At the detector the THz pulse and gate pulse are overlap spatially and temporally. The timing between both pulses is adjusted via a delay line.

The used THz-TDS system is illustrated in Figure 3. The output of a femtosecond laser is split into THz generation and gating pulses. The generation uses a photo-conductive switch. This switch is opened and biased without laser excitation. The laser pulse generates free charges in the switch, dramatically increasing the conductivity and closing the switch. The biased and closed switch gives rise to a short current pulse. This current pulse in turn emits THz radiation. The THz beam is routed via four off-axis parabolic mirrors, focusing the beam on the sample and refocusing the transmitted radiation on the receiving antenna. The receiver is again based on a photoconductive switch. This second switch is not biased externally. The electrical field of the focused THz radiation creates a local bias on the switch. The gating pulse closes the switch and the THz radiation that is present at that time drives a current across the switch. This current can be measured with slow electronics; the time resolution is achieved by the laser pulse duration and the carrier lifetime within the photoconductive switch. A mechanical delay line is used to adjust the timing between gating and THz pulses, allowing for femtosecond resolved mapping of the THz pulse. For the experiments presented here, samples were mounted in a liquid nitrogen cooled cryostat. Each sample was also placed on a micrometer positioning stage allowing us to verify the homogeneity of the sample.

# 4. THZ CONDUCTIVITY IN Mn<sub>2</sub>DSBDC

#### 4.1 Data Processing

The dry-MOF powder was mixed with Teflon in a mixing ration of 0.02:1. The low concentration ensured that low-loss approximations can be used to determine the complex refractive index of the mixture. <sup>12</sup> Effective medium theory <sup>13</sup> was used to calculate the properties of the MOF from the known properties of the host (Teflon) and the measured properties of the mixture. The complex refractive index of a material can always be written as:

$$n = \sqrt{(\epsilon \mu)} \approx \sqrt{(\epsilon)} \tag{1}$$

$$\epsilon = \epsilon_{\text{lattice}} \epsilon_0 - \frac{i\sigma}{\omega} \tag{2}$$

With  $\epsilon$  and  $\mu \approx 1$  denoting the complex permittivity and permeability, respectively.  $\sigma$  refers to the complex conductivity and  $\epsilon_{\text{lattice}}$  describes the complex permittivity contribution from bound charges in the lattice.

The remaining challenge is to accurately separate the lattice contribution from the conductivity. Without additionally knowledge of the material or assumptions this is impossible. Hence, we made the assumption that the permittivity of the sample follows the Drude-Smith model: $^{14-16}$ 

$$\epsilon(\omega) = \epsilon_{\text{lattice}} - \left[ \left( \frac{\tau \omega_p^2}{\tau \omega_p + i\omega} \right) \left( 1 + \frac{c}{1 - i\omega\tau} \right) \right]$$
 (3)

With  $\omega_p$  denoting the plasma frequency,  $\tau$  the scattering time, and c the c-parameter. The c-parameter describes how likely an electron is transferred from one grain to another, with 0 meaning no hindering and -1 a full localization.

#### 4.2 Drude Conductivity in Mn<sub>2</sub>DSBDC

The conductivity of  $Mn_2DSBDC$  for different temperatures is plotted in Figure 4 a). We directly notice that the conductivity for different temperatures is unchanged within the error bars. This is a striking result. Most conductivity mechanisms, like those involving dopants or thermally activated hopping, strongly depend on the temperature. Also, phonon scattering scales exponentially with thermal energy. The fact that the conductivity in  $Mn_2DSBDC$  is rather independent of the temperature is a clear indicator that the underlying mechanism of conductivity is not based on either of the aforementioned processes.

The conductivity for MOFs with different dopants also did not show a clear temperature trend (not shown here). As a representative temperature, 300 K was chosen and the results are plotted in Figure 4 b). The most important result of these experiments is that the dopant does not disturb the conductivity of the MOF. This is crucial as it verifies that catalytically relevant metals can be incorporated without destroying the conductivity.

The aforementioned Drude Smith fits yielded an excellent agreement with the experimental data. The c-parameter of the fits to the pure and the doped materials for 300 K, 200 K and 100 K is between -0.9 and -1. The c-parameter close to -1 indicates a strongly suppressed inter-grain conductivity, while 0 corresponds to an unhindered flow of electrons as observed in single crystalline bulk.

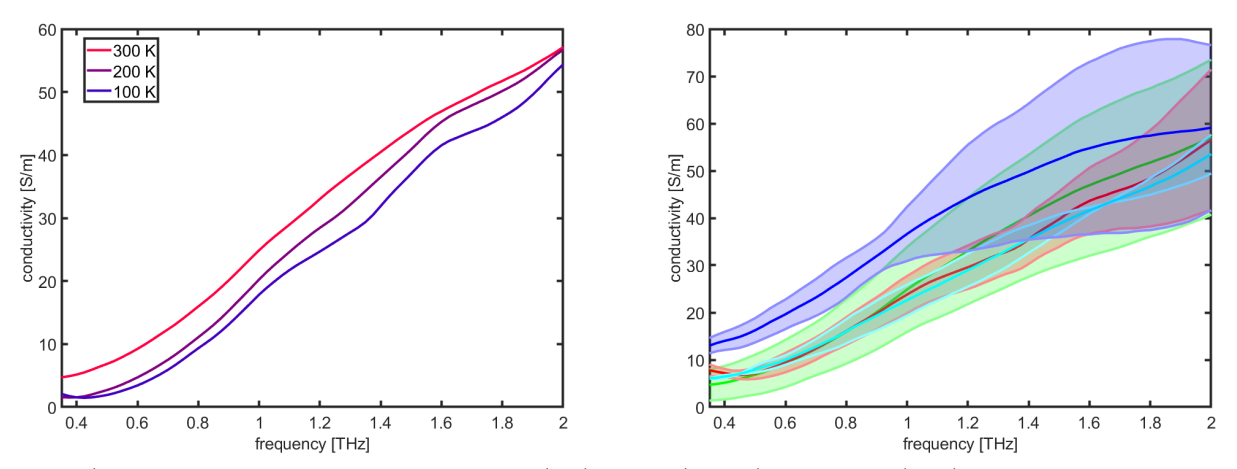


Figure 4. a) Conductivity of  $Mn_2DSBDC$ , for 300 K (red), 200 K (purple), and 100 K (blue). No clear temperature trend prevails when error bars are considered. b) Conductivity of  $Mn_2DSBDC$  (green) and for Cu- $Mn_2DSBDC$  (red), Co- $Mn_2DSBDC$  (cyan), and Ni- $Mn_2DSBDC$  (blue) at 300 K. Within the measurement uncertainty all MOF conductivities overlap.

# 5. PUMP PROBE SPECTROSCOPY OF Zn<sub>2</sub>TTFTB

As a final result highlighted in this presentation, we studied  $Zn_2TTFTB-MOF$ . Unlike  $Mn_2DSBDC$ ,  $Zn_2TTFTB$  exhibits photoconductivity in our THz measurements. Photoconductivity is a crucial requirement for photo-driven catalysis and as such determining the photoconductivity of MOFs is a crucial step to benchmark their potential for light-driven applications.

The MOF was synthesized as described in Narayan et al.<sup>17</sup> The sample was measured using optical pump THz probe (OPTP) spectroscopy, <sup>18, 19</sup> a technique that adds an ultrafast photoexcitation to the previously discussed THz-TDS. The additional pump-probe time delay is used to understand the dynamics following an ultrashort photoexcitation. On the THz time axis, the THz-Gate delay time is adjusted to monitor the THz field-peak in time domain. The pump-probe delay is then scanned and the THz-transmittance difference between photoexcited and non-excited is collected. The resulting OPTP trace is plotted in Figure 5.

The measured OPTP highlights the outstanding strength of THz spectroscopy. The sub-picosecond time resolution of OPTP allowed us to determine the decay constant of three distinct processes. The first exhibit an ultrafast decay of 0.6 ps, the second a decay with 31 ps and the third was fixed at 10 ns, which is longer than our maximum delay. This long living excitation was previously reported using microwave conductivity techniques.<sup>17</sup> However, microwave techniques are blind for the ultrafast processes detected via OPTP. These processes, however, can be crucial for chemical reactions as the shorter time frames might still be sufficiently long lived to reach a catalytical side and deposit their photoenergy into the desired chemical reaction.

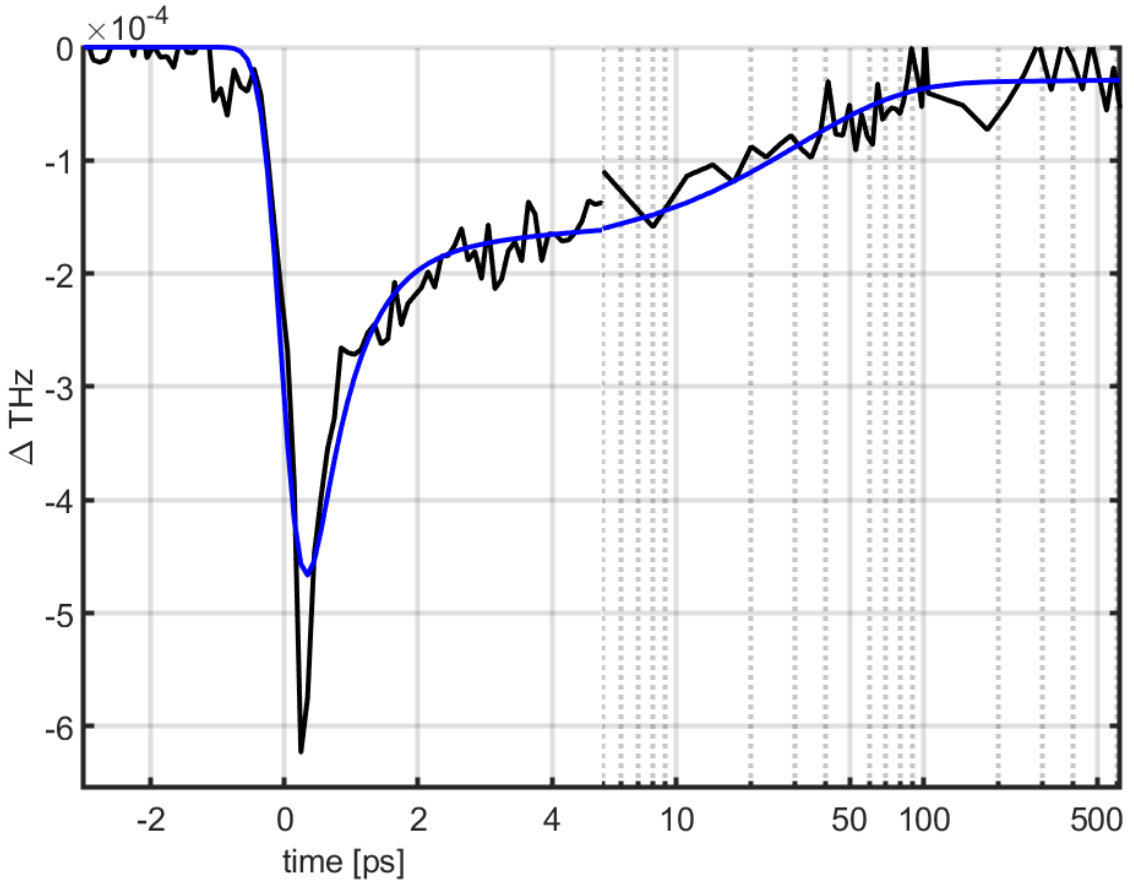


Figure 5. Optical Pump THz Probe (OPTP) traces of  $Zn_2TTFTB$ , pumped at 400 nm. The experimental data (black) was fitted with a triple exponential function (blue).

#### 6. CONCLUSION

THz time domain spectroscopy (THz-TDS) and optical pump THz probe (OPTP) spectroscopy have been previously demonstrated for a large range of materials, ranging from semiconductors to nanoparticles. Our group demonstrated that these techniques can also be leveraged to gain insight into metal organic frameworks (MOFs).

We measured the ground state conductivity in  $\rm Mn_2DSBDC$ . The conductivity at 1 THz exceeded 10 S/m, significantly higher than previously reported values of 0.25 pS/m. <sup>20</sup> The higher conductivity at high frequency is a strong indicator that the overall DC conductivity is limited by inter grain conductivity, which is less pronounced at higher frequencies. This insight can be used to improve material properties.

We also demonstrated the superior time resolution of OPTP compared to time resolved microwave conductivity (TRMC). The measured ultrafast decay times of 0.6 ps and 31 ps were much faster than previously reported values from TRMC experiments which lack subpicosecond time resolution. This highlights OPTPs strength in understanding conductivity on the sub-ps scale, which in turn can provide a guide towards designing superior photo-harvesting materials.

#### ACKNOWLEDGMENTS

We appreciate the support from the Energy Science Institute (ESI) and the Microbial Science Institute (MSI) and our colleagues therein. We are also grateful for funding from NSF under grant number CHE-1954453.

#### REFERENCES

- Tachibana, Y., Vayssieres, L., and Durrant, J. R., "Artificial Photosynthesis for Solar Water-Splitting," Nat. Photonics 6, 511 (2012).
- [2] Young, K. J., Martini, L. A., Milot, R. L., Snoeberger, R. C., Batista, V. S., Schmuttenmaer, C. A., Crabtree, R. H., and Brudvig, G. W., "Light-Driven Water Oxidation for Solar Fuels," Coord. Chem. Rev. 256(21), 2503 2520 (2012). Solar Fuels- by invitation only.
- [3] Neu, J., Ostresh, S., Regan, K. P., Spies, J. A., and Schmuttenmaer, C. A., "Influence of Dye Sensitizers on Charge Dynamics in SnO<sub>2</sub> Nanoparticles Probed with THz Spectroscopy," J. Phys. Chem. C 124(6), 3482–3488 (2020).
- [4] CCSD, "MOF Subset of The Cambridge Crystallographic Data Centre (CCDC)," (Version 5.38).
- [5] Pattengale, B., Neu, J., Ostresh, S., Hu, G., Spies, J. A., Okabe, R., Brudvig, G. W., and Schmuttenmaer, C. A., "Metal-Organic Framework Photoconductivity via Time-Resolved Terahertz Spectroscopy," J. Am. Chem. Soc. 141(25), 9793–9797 (2019).
- [6] Xie, L. S., Skorupskii, G., and Dincă, M., "Electrically Conductive Metal-Organic Frameworks," Chem. Rev. (2020).
- [7] Sun, L., Campbell, M. G., and Dincă, M., "Electrically Conductive Porous Metal-Organic Frameworks," Angew. Chem. Int. Ed. 55(11), 3566-3579 (2016).
- [8] Sun, L., Miyakai, T., Seki, S., and Dinca, M., "Mn2(2,5-disulfhydrylbenzene-1,4-dicarboxylate) A Microporous Metal-Organic Framework with Infinite Mn-S Chains and High Intrinsic Charge Mobility," J. Am. Chem. Soc. 135(22), 8185–8188 (2013).
- [9] Neu, J. and Schmuttenmaer, C. A., "Tutorial: An Introduction to Terahertz Time Domain Spectroscopy (THz-TDS)," J. Appl. Phys. 124(22), 231101 (2018).
- [10] Neu, J., Regan, K., Swierk, J. R., and Schmuttenmaer, C. A., "Applicability of the Thin-film Approximation in Terahertz Photoconductivity Measurements," Appl. Phys. Lett. 113(22), 233901 (2018).
- [11] Grischkowsky, D., Duling III, I. N., Chen, J. C., and Chi, C. C., "Electromagnetic shock waves from transmission lines," *Phys. Rev. Lett.* **59**, 1663–1666 (1987).
- [12] Neu, J., Stone, E. A., Spies, J. A., Storch, G., Hatano, A. S., Mercado, B. Q., Miller, S. J., and Schmuttenmaer, C. A., "Terahertz Spectroscopy of Tetrameric Peptides," *J. Phys. Chem. Lett.* **10**(10), 2624–2628 (2019).

- [13] Markel, V. A., "Introduction to the Maxwell Garnett Approximation: Tutorial," J. Opt. Soc. Am. A 33(7), 1244–1256 (2016).
- [14] Cocker, T. L., Baillie, D., Buruma, M., Titova, L. V., Sydora, R. D., Marsiglio, F., and Hegmann, F. A., "Microscopic Origin of the Drude-Smith Model," *Phys. Rev. B* **96**(20), 205439 (2017).
- [15] Smith, N. V., "Classical Generalization of the Drude Formula for the Optical Conductivity," *Phys. Rev.* B **64**(15), 155106 (2001).
- [16] Krewer, K. L., Ballabio, M., and Bonn, M., "The Drude-Smith Model for Conductivity: de novo Derivation and Interpretation," (2020).
- [17] Narayan, T. C., Miyakai, T., Seki, S., and Dincă, M., "High Charge Mobility in a Tetrathiafulvalene-Based Microporous Metal-Organic Framework," J. Am. Chem. Soc. 134(31), 12932–12935 (2012).
- [18] Beard, M. C., Turner, G. M., and Schmuttenmaer, C. A., "Transient Photoconductivity in GaAs as Measured by Time-Resolved Terahertz Spectroscopy," *Phys. Rev. B* **62**(23), 15764–78 (2000).
- [19] Neu, J. and Rahm, M., "Terahertz Time Domain Spectroscopy for Carrier Lifetime Mapping in the Picosecond to Microsecond Regime," Opt. Express 23(10), 12900–12909 (2015).
- [20] Park, S. S., Hontz, E. R., Sun, L., Hendon, C. H., Walsh, A., Van Voorhis, T., and Dincă, M., "Cation-Dependent Intrinsic Electrical Conductivity in Isostructural Tetrathiafulvalene-Based Microporous Metal-Organic Frameworks," J. Am. Chem. Soc. 137(5), 1774–1777 (2015).